Diffusion- and drift-controlled reactions in two and three dimensions

G. J. Sibona and C. E. Budde
Facultad de Matemática, Astronomía y Física, Universidad Nacional de Córdoba, Ciudad Universitaria, 5000 Córdoba, Argentina

C. A. Condat
Department of Physics, University of Puerto Rico, Mayagüez, Puerto Rico 00681

(Received 20 May 1996)

We analyze the steady state of a reaction in which mobile reactants diffusing under the action of a uniform field may be absorbed by perfect or imperfect spherical traps. We obtain contour maps for the concentration and for the probability distribution function for the first mobile neighbor of the trap. This permits a clear visualization of the effects of a trap on the statistics of the mobile particles. We also obtain the trapping (or reaction) rates for the two- and three-dimensional problems, and examine the influence of drift and trapping strength. While in the absence of a field there is no steady state in two dimensions, we show here that the addition of an arbitrarily small field suffices to make it possible. In the small-field limit, the reaction rate vanishes as $|\ln(V/D)|^{-1}$, where V is the drift velocity and D is the diffusion coefficient. [S1063-651X(96)11812-2]

PACS number(s): 05.40.+j, 66.10.Cb, 66.30.−h, 82.20.−w

I. INTRODUCTION

The analysis of nearest-neighbor distances in diffusion-controlled reactions has received considerable attention in the last few years [1–4]. In these studies a uniformly distributed set of random walkers A is assumed to be diffusing in the neighborhood of a fixed (perfect or imperfect) trap B. Due to trapping, a gradient of species A appears near the trap [5,6]. The resulting perturbed region can be described in terms of the probability density function (PDF) $f(L,t)$ for the nearest-neighbor distance L to the trap. Using this function, it was shown that the average distance from the trap to its nearest neighbor increases asymptotically as $\langle L\rangle \sim t^{1/4}$ in one dimension [2,3], and as $\langle L\rangle \sim (\ln t)^{1/2}$ in two dimensions [4]. In three dimensions a steady state is reached at long times [2,3].

The results mentioned in the preceding paragraph hold when the diffusion of the A particles is completely unbiased. On the other hand, diffusion-controlled reactions in the presence of biasing fields are of great interest in many areas. Let us briefly mention a few instances: (a) In positron tomography [7], the addition of a strong electric field perpendicular to the surface leads to greater sample penetration, allowing for the investigation of regions situated farther away from the surface. (b) In the problem of electromigration [8], the model discussed in this paper could be used to analyze the effect of trapping centers on carrier concentration. (c) The analysis of wetting layer growth at the surface of a critical mixture requires the consideration of the diffusion of the wetting molecules under the action of a uniform gravitational field [9], while the surface acts as a trap. (d) Gravity is also responsible for the drift of water molecules diffusing underground [10,11]. The distribution of water near underground cavities turns out to be closely related to the results generated by our model for the special case of impenetrable obstacles. (e) Finally, in order to understand the phenomenon of particle segregation due to shaking in a gravitational field, Alexander and Lebowitz considered driven diffusive flow past an impenetrable obstacle in both the continuum and lattice versions [12].

Recently, we analyzed the effects of a uniform field on the distribution of mobile particles in one dimension, showing that a steady state is reached exponentially fast if the field points towards the trap, while the depletion hole grows rapidly if the field points away from the trap [13].

In the absence of a bias, the two-dimensional problem is clearly marginal. Any mechanism that contributes to replenishing the depletion hole should lead to the existence of a steady state. A uniform field that continuously brings A particles to the trap neighborhood is one such mechanism. In this paper we consider the effects of a uniform field on the distribution of nearest-neighbor distances in two and three dimensions. We will analyze the nature of this steady state, indicating how it evolves when field intensity and trap strength are modified. We will also compute the steady-state reaction rate at the trap, which we expect to be a monotonically increasing function of field intensity and trap strength. Of particular interest is the small bias limit in the two-dimensional problem. In this case we obtain an approximate analytical expression for the steady-state concentration. We also show that the steady-state reaction rate vanishes as $|\ln(V/D)|^{-1}$, where V is the drift velocity and D is the diffusion coefficient.

It is interesting to note that a related model for diffusion-controlled reactions, the so-called ''trapping'' model, in which a particle diffuses in a medium containing a random distribution of traps, leads to very different results. For this model, the asymptotic survival probability $S(t)$ is given by a stretched exponential $S(t)\sim \exp(-kt^{d/(d+2)})$, where k is a constant and d is the system dimension [14]. Instead of favoring a steady state, the addition of a field speeds up particle annihilation, leading to a simple exponential decay for $S(t)$ [15,16].

After introducing our model in Sec. II, in Sec. III we present an elementary discussion of the relation between the field and the steady state in two dimensions. This is a point

that does not seem to have been remarked upon in the literature. In Sec. IV we calculate the steady-state solution for the concentration. An analytical solution is possible only in the case of perfect traps. For imperfect traps we have developed a simple algorithm that permits a rapid evaluation of the solution for arbitrary values of the parameters. In Secs. V and VI we study the steady-state statistical properties of the nearest-neighbor distances to the trap and the reaction rates, respectively. Using the procedure introduced in Sec. IV, we analyze the small-field limit in Sec. VII.

II. MODEL

The underlying hypothesis is that the density of fixed reactants (traps) is low, so that we may neglect the interactions between their regions of influence. We may then assume that an imperfect trap of radius a is located at the origin. Trapping occurs with a conditional rate γ given that a mobile particle has reached the trap edge. We further assume that the mobile particles are initially distributed in space with a uniform concentration C_0, and that the constant field is applied in the direction of the negative z axis. Under these conditions the position and time dependence of the concentration at $t>0$ can be found by solving the diffusion equation with a bias,

$$\frac{\partial C}{\partial t}=D\nabla^2 C+V\frac{\partial C}{\partial z}, \tag{1}$$

subject to the radiation boundary condition

$$D\frac{\partial C}{\partial r}\bigg|_{r=a}=(\gamma-V\cos\theta)C|_{r=a}, \tag{2}$$

where r is the radial distance and θ is the angle measured with respect to the z direction. It is convenient to introduce the dimensionless time $\tau=Dt/a^2$ and radial distance $\xi=r/a$. The discussion is also simplified if we use the dimensionless drift velocity $W=Va/2D$ and trapping rate $\Gamma=\gamma a/D$.

III. EXISTENCE OF A TWO-DIMENSIONAL STEADY STATE

Why does a steady state arise in two dimensions when a small field is applied? Before working out the solution to the model introduced in Sec. II, we wish to present a simple argument to show that a steady state is possible for an arbitrary finite trap if a field is present. First, we note that, in the absence of a field, a steady-state solution of Eq. (1) must be of the form

$$C_\infty(\xi,\theta)=[a+b\ln(\xi)]f(\theta). \tag{3}$$

If we demand that $C_\infty(\xi\to\infty)=C_0$, then $b=0$. This restriction makes it impossible to find a steady-state solution that also satisfies boundary conditions for a finite trap of any shape (the exception is, of course, the perfect reflector, $\Gamma=0$). However, since the logarithm diverges more slowly than any power for large values of the argument, it is reasonable to expect that any perturbation that favors the displacement of particles from very long distances must lead to a steady state. This can be seen most easily using dimensionless Cartesian coordinates (χ,ζ). The equation satisfied by the steady state is then,

$$\frac{\partial^2 C_\infty}{\partial\chi^2}+\frac{\partial^2 C_\infty}{\partial\zeta^2}+2W\frac{\partial C_\infty}{\partial\zeta}=0. \tag{4}$$

Writing $C_\infty(\chi,\zeta)=C_o+X(\chi)Z(\zeta)$, and applying the boundary condition at infinity, it is clear that the solution must be a superposition of functions of the form

$$e^{-\alpha|\chi|}e^{-(w\pm\Delta)|\zeta|},$$

where $\Delta=\sqrt{W^2-\alpha^2}$, with α being the separation constant. We conclude the following,

(1) If $W=0$, Δ is imaginary and $Z(\zeta)$ purely oscillatory; the condition at $\zeta\to\infty$ cannot be fulfilled: No steady state is possible.

(2) If $W\neq0$, then all the components contain an exponentially decreasing function. The exponential is present for any value of $W\neq0$, regardless of how small, and makes the steady state possible. Of course, the larger the value of W, the faster the solution tends to its asymptotic value.

(3) The previous observations do not have anything to do with the trap. They are therefore valid for all trap shapes and sizes (if finite). The boundary conditions at the trap edge only determine the contribution of each component to the solution.

IV. STEADY-STATE CONCENTRATION

The one-dimensional version of our model was solved and discussed in Ref. [13]. In this section we present the solution for the steady-state concentration in two and three dimensions.

Following Smoluchowski [5] and Carslaw and Jaeger [17], we introduce a function u [such that $u(\tau=0)=0$], given by

$$C=C_0(1+ue^{W\zeta}), \tag{5}$$

where $\zeta=z/a$ is the dimensionless distance along the direction of the field. We perform a Laplace transform $[u(\tau)\to\tilde{u}(s)]$. In terms of the function $\tilde{u}(s)$, Eqs. (1) and (2) read

$$\nabla^2\tilde{u}-q^2\tilde{u}=0 \tag{6}$$

and

$$\frac{\partial\tilde{u}}{\partial\xi}\bigg|_{\xi=1}=(\Gamma-W\cos\theta)\tilde{u}+(\Gamma-2W\cos\theta)\frac{1}{s}e^{W\cos\theta}, \tag{7}$$

where $q^2=W^2+s$ and ∇^2 stands now for the dimensionless Laplacian.

Next we obtain the steady-state solution of these equations.

A. Two-dimensional case ($d=2$)

Following Ref. [17] we separate variables in Eq. (6) and write

$$\tilde{u}(\xi,\theta;s)=\sum_{j=0}^{\infty}\frac{\alpha_j}{s}\cos(j\theta)K_j(q\xi), \tag{8}$$

with the K_j's being the modified Bessel functions of the second kind [18]. The coefficients α_j are found by using the boundary condition Eq. (7), in which the exponential in the last term is expanded in terms of the modified Bessel functions of the first kind, I_n,

$$e^{W\cos\theta}=I_0(W)+2\sum_{n=1}^{\infty}I_n(W)\cos(n\theta). \tag{9}$$

Equating the coefficients in the cosine expansion, we find the relation

$$q\alpha_jK_j'(q)-\Gamma\alpha_jK_j(q)+(W/2)[\alpha_{j-1}K_{j-1}(q)+\alpha_{j+1}K_{j+1}(q)]=B_j, \tag{10}$$

with

$$B_0=\Gamma I_0(q)-2WI_1(q)$$

and

$$B_j=2\{\Gamma I_j(q)-W[I_{j-1}(q)+I_{j+1}(q)]\}, \tag{11}$$

if $j>0$.

For a perfect trap ($\Gamma\to\infty$), Eq. (10) yields

$$\alpha_j=-\frac{\epsilon_jI_j(q)}{K_j(q)}, \tag{12}$$

with $\epsilon_j=2-\delta_{j0}$. A full analytical solution is then possible. By taking the inverse Laplace transform and then the long-time limit, Carslaw and Jaeger [17] obtained the steady-state solution $C_\infty(\xi,\theta)$,

$$C_\infty(\xi,\theta)=C_0\left[1-e^{-W\xi\cos\theta}\sum_{j=0}^{\infty}\frac{I_j(W)}{K_j(W)}\epsilon_jK_j(W\xi)\cos(j\theta)\right]. \tag{13}$$

At long distances from the trap, we obtain the result

$$C_\infty(\xi,\theta)=C_0\left[1-\left(\frac{\pi}{2W\xi}\right)^{1/2}e^{-W\xi(1+\cos\theta)}F(\theta,W)\right], \tag{14}$$

where $F(\theta,W)$ does not depend on the distance ξ. As we increase ξ, the steady-state solution goes exponentially fast to its asymptotic value, except in the direction $\theta=\pi$, for which the convergence goes only as $\xi^{-1/2}$; this shows that the shadow extends very far behind the trap.

The high field result is also of some interest. If $W\gg1$, Eq. (13) leads to

$$C_\infty(\xi,\theta)=C_0[1-\xi^{-1/2}e^{-W(\xi-1)(1+\cos\theta)}], \tag{15}$$

which satisfies the boundary condition $C_\infty(1,\theta)=0$, and goes exponentially fast to the asymptotic result (except, again, for the $\theta=\pi$ direction).

For a partially absorbing trap an analytical solution is not possible. We will therefore develop a numerical method to obtain the desired results. Equation (10) can be written in matrix form as

$$\mathcal{M}\vec{\alpha}=\vec{B}, \tag{16}$$

where $\vec{\alpha}$ is the column vector formed by the α_j's, and $\vec{B}$ is the column vector whose components are given by Eq. (11). The elements of the matrix $\mathcal{M}$ are

$$\mathcal{M}_{i,i}=qK_i'(q)-\Gamma K_i(q),$$

$$\mathcal{M}_{i,i+1}=\frac{W}{2}K_{i+1}(q), \tag{17}$$

$$\mathcal{M}_{i+1,i}=\frac{W}{2}(1+\delta_{i0})K_i(q).$$

We can now find the α_j's by numerical inversion of $\mathcal{M}$, i.e.,

$$\vec{\alpha}=\mathcal{M}^{-1}\vec{B}. \tag{18}$$

High precision is achieved using a relatively small number of components. Since we are interested only in the steady state (the long-time limit), we may take $q=W$.

In all the figures in this paper we will assume that the concentration at infinity takes the value $C_0=0.25$. Contour maps of the steady-state concentration are shown in Fig. 1 for $W=0.5$ and two values of the absorption rate Γ. Figure 1(a) corresponds to an impenetrable trap; no reaction occurs. Figure 1(b) corresponds to a more efficient trap. Note that, with the chosen sign for the drift velocity, the current is coming from the right. Further information is obtained by plotting the steady-state concentration along particular directions. A plot of the concentration along the field (ζ) axis is shown in Fig. 2 for $W=0.5$ and $\Gamma=0$ (a) and 1 (b). Several features of the graphs are evident.

(a) The depletion region behind the trap increases in range and depth with Γ.

(b) If $\Gamma<\infty$, some of the particles hitting the trap wall are reflected. This leads to an enhancement of the upstream concentration. If Γ is low enough, this concentration becomes higher than C_0 in the trap neighborhood; this effect is stronger at high drift.

(c) Another consequence of the reflection at the trap wall is the apparition of enhanced concentration lobes about the trap. This was first noticed for the case of perfectly reflecting obstacles ($\Gamma=0$) in the work of the Australian group on unsaturated seepage and subterranean holes, for which the drift is due to gravity [10]. At large drifts, the enhanced concentration lobes extend a large distance downstream, while the disturbed region in front of the trap becomes very thin. Of course, for a perfect trap ($\Gamma=\infty$), $C=0$ at the trap edge and no lobes appear.

By taking the limit $W\to0$, it is easy to reobtain Taitelbaum's result in the $t\to\infty$ limit [see Eq. (3) in Ref. [4]] which, as was mentioned before, does not lead to a steady state. However, since $W=0$ is a marginal case in two dimensions, a steady-state solution must exist for all $W\neq0$. In

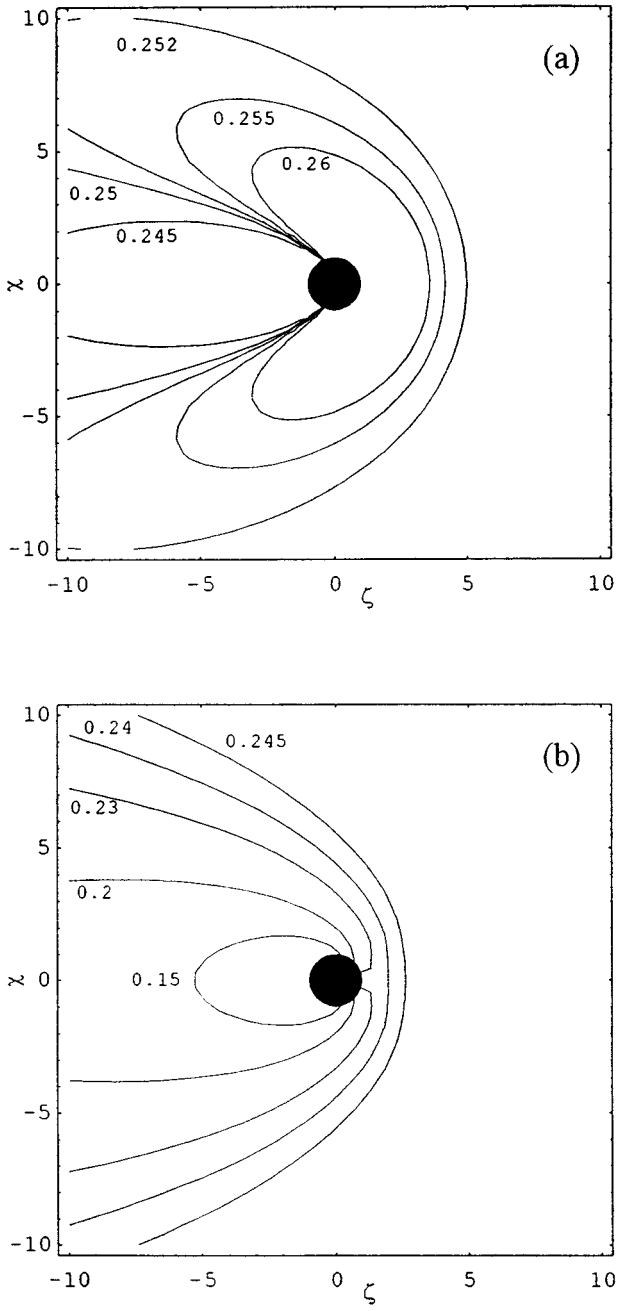

FIG. 1. Concentration contour plots ($d=2$). In all figures the trap radius is unity, and $C_0=0.25$. Here $W=0.5$ and $\Gamma=0$ (a) and $\Gamma=1$ (b).

Sec. III we showed how the presence of a field introduces a factor that decays exponentially in space. This allows for the fulfillment of the boundary condition at infinity for any finite trap size or shape, which makes the steady state possible. It is easy to generate a steady-state concentration contour plot for a ''nearly marginal'' case (say, $W\sim 10^{-11}$). On the scale of Fig. 1 such a plot would look perfectly symmetric, as if no field were present. However, in practice it may take a very long time for this steady state to be reached.

We conclude the analysis of the steady-state concentration in two dimensions by presenting a high-field ($W=2.5$) contour plot, where we can observe the downstream prolongation of the high concentration lobes (see Fig. 3).

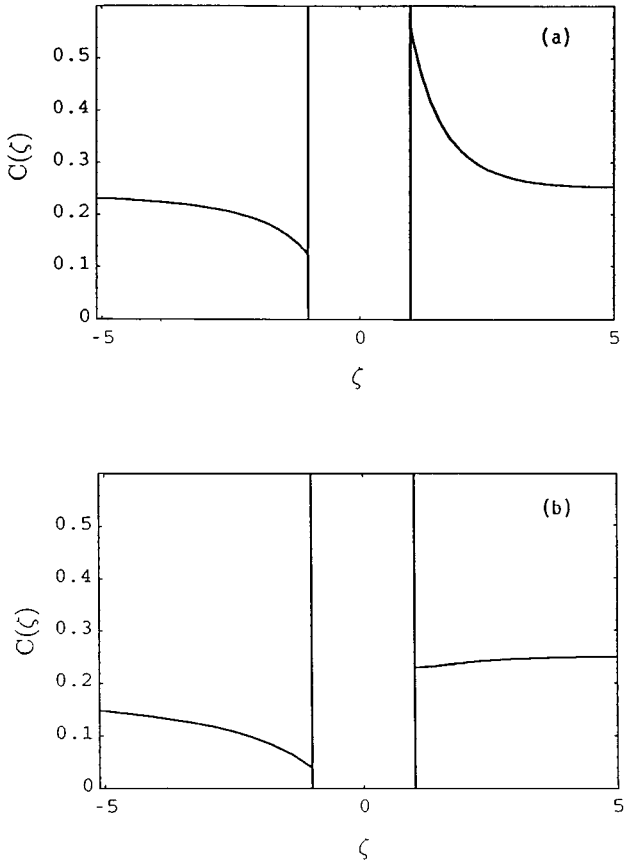

FIG. 2. Concentration along the ζ axis ($d=2$). Here $W=0.5$ and $\Gamma=0$ (a) and $\Gamma=1$ (b). Note the depletion and enhancement regions behind and in front of the trap, respectively.

B. Three-dimensional case ($d=3$)

In the three-dimensional case the separation of variables in Eq. (6) leads to

$$\tilde{u}(\xi,\theta,\phi)=\sum_{j=0}^{\infty}\frac{\alpha_j}{s}\frac{K_{j+1/2}(q\xi)}{\xi^{1/2}}P_j(\cos\theta), \tag{19}$$

where ϕ is the azimuthal angle and P_j are the Legendre polynomials. Next we expand the last term of Eq. (7) in terms of P_j,

$$(\Gamma-2W\cos\theta)e^{W\cos\theta}=\sum_{n=0}^{\infty}B_nP_n(\cos\theta), \tag{20}$$

with the coefficients

$$B_n=\frac{2n+1}{2}\int_{-1}^{1}dxP_n(x)(\Gamma-2Wx)e^{Wx}. \tag{21}$$

Substituting Eqs. (19) and (20) into Eq. (7), we again obtain an equation having the form (16). The matrix elements of $\mathcal{M}$ are now

$$\mathcal{M}_{i,i}=K_{i+1/2}(q)\left[q\frac{K'_{i+1/2}(q)}{K_{i+1/2}(q)}-\Gamma-\frac{1}{2}\right], \tag{22}$$

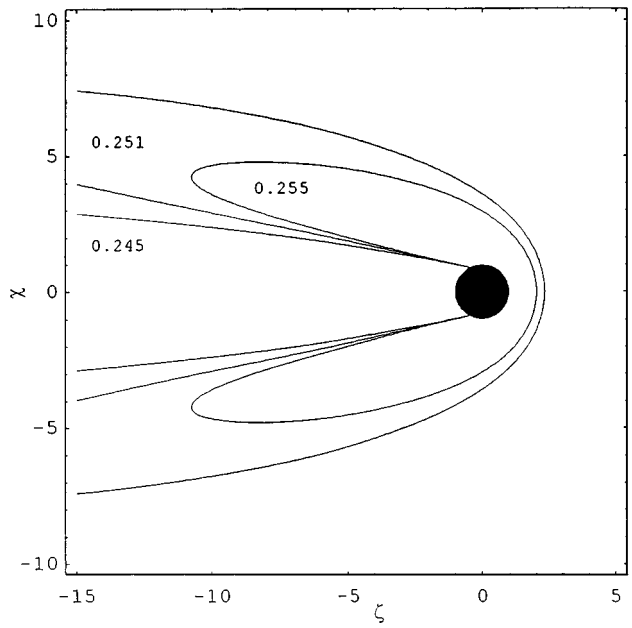

FIG. 3. Concentration contour plot ($d=2$) for $\Gamma=0.1$ and $W=2.5$.

$$\mathcal{M}_{i,i+1}=\frac{W(i+1)}{2i+3}K_{i+3/2}(q),$$

$$\mathcal{M}_{i+1,i}=\frac{W(i+1)}{2i+1}K_{i+1/2}(q).$$

An analytical solution is again possible for the perfect trap ($\Gamma\to\infty$). In the asymptotic long-time limit, we take $s\to 0$ and, consequently, $q\to W$. The inverse Laplace transform leads to the steady-state solution

$$C_\infty(\xi,\theta)=C_0\left[1-\left(\frac{\pi}{2W\xi}\right)^{1/2}e^{-W\xi\cos\theta}\sum_{j=0}^{\infty}(2j+1)\times\frac{I_{j+1/2}(W)}{K_{j+1/2}(W)}K_{j+1/2}(W\xi)P_j(\cos\theta)\right]. \quad (23)$$

At long distances from the trap, we again obtain an equation having the form of Eq. (14), but with ξ^{-1} replacing $\xi^{-1/2}$ in the prefactor. The same can be said about the high-field limit and Eq. (15). The $W\to 0$ limit will be examined in Sec. VII.

For imperfect traps, we can use Eq. (23) to obtain steady-state concentration contour maps. Figures 4 and 5 are the counterparts of Figs. 1 and 3 for a three-dimensional system. The concentration is axially symmetric with respect to the field axis. Although we observe the same general features in the two- and three-dimensional problems, the intensity of the disturbance generated by the presence of the trap is noticeably weaker in the three-dimensional case. There are more ways for particles to replenish the depleted region near the trap, and there are more ways for the particles reflected at an imperfect trap to leave the enhanced concentration region. For this reason, we may speculate that the disturbed region would become very small for high-dimensionality systems, being confined to a thin boundary layer about the trap.

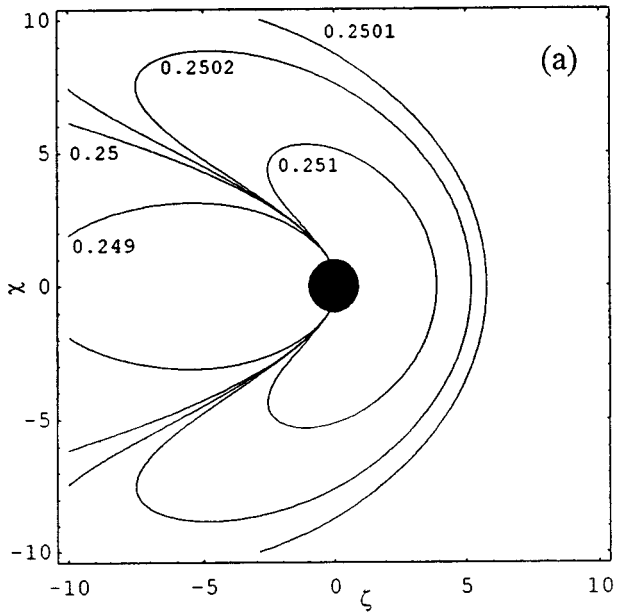

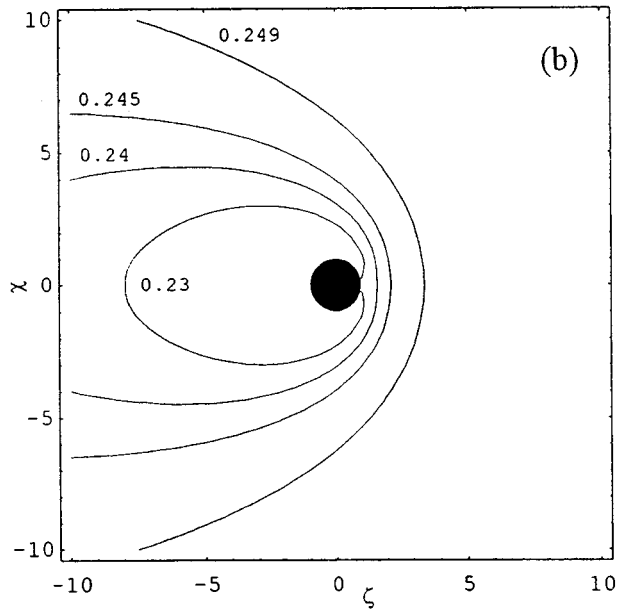

FIG. 4. Concentration contour plots ($d=3$). Here $W=0.5$ and $\Gamma=0$ (a) and $\Gamma=1$ (b). The concentration has a cylindrical symmetry about the ζ axis.

V. NEAREST-NEIGHBOR DISTANCES

The interest in the statistical properties of nearest-neighbor distances in diffusion problems has been rekindled by the work of Ben-Avraham and co-workers [1,2,19,20]. In this section we evaluate the steady-state statistical properties of the nearest-neighbor distances to the trap. The probability that the nearest diffusing particle is at a (dimensionless) distance larger than L from the trap in the direction specified by the solid angle Ω is given by

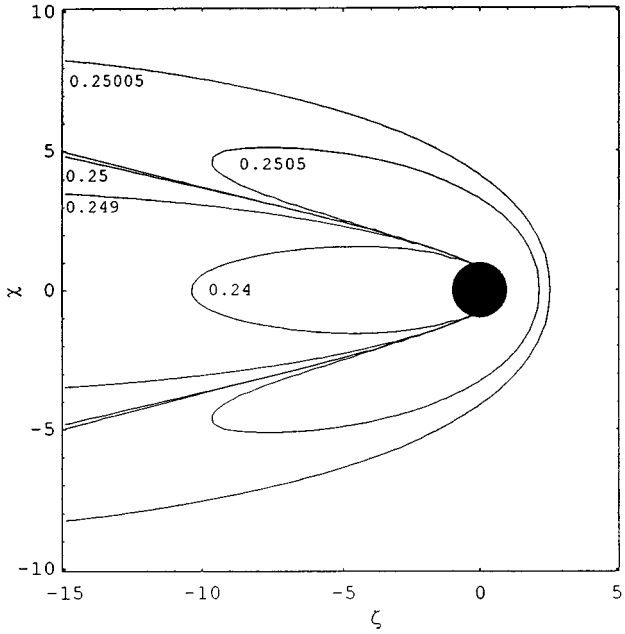

FIG. 5. Concentration contour plot ($d=3$) for $\Gamma=0.1$ and $W=2.5$. The concentration has a cylindrical symmetry about the ζ axis.

$$\Phi(L,\Omega)=e^{-a^d\int_1^L d\xi\xi^{d-1}C_\infty(\xi,\theta)}, \tag{24}$$

where d is the system dimension. Despite the axial symmetry around the polar axis, we write explicitly the full angular dependence to stress that the solid angle is fixed. The probability distribution function (PDF) of the distance from the trap to the nearest mobile particle in the direction Ω can be calculated by taking the derivative

$$f(L,\Omega)=-\frac{\partial\Phi(L,\Omega)}{\partial L}. \tag{25}$$

This PDF satisfies the normalization condition

$$\int_1^\infty f(L,\Omega)dL=1. \tag{26}$$

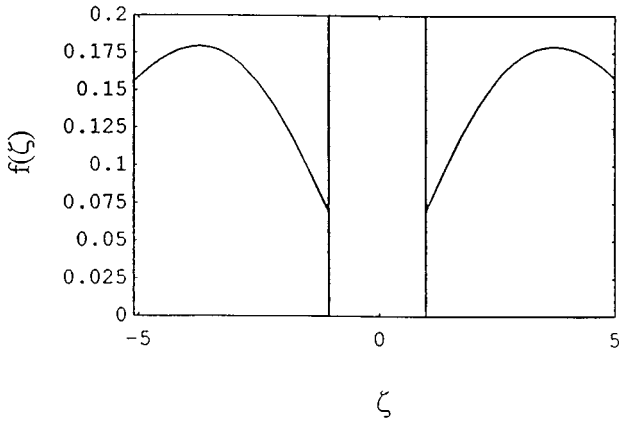

FIG. 6. A cut of the PDF along the ζ axis for the $d=2$ problem with $\Gamma=0.1$ and $W=5\times10^{-12}$. In the scale of the figure the PDF has circular symmetry.

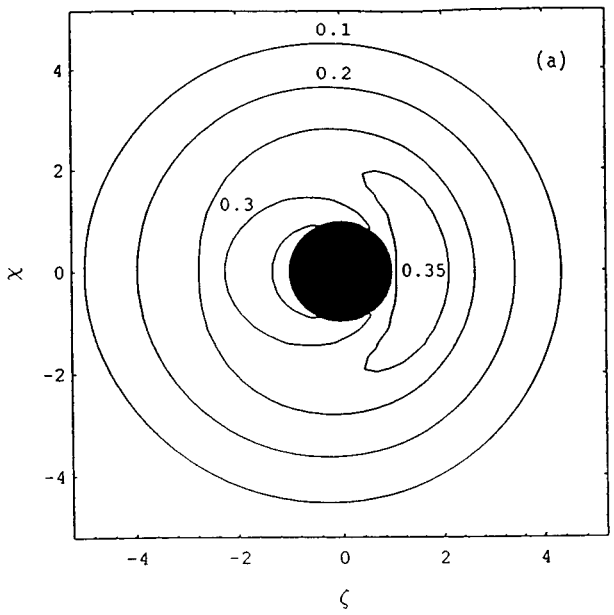

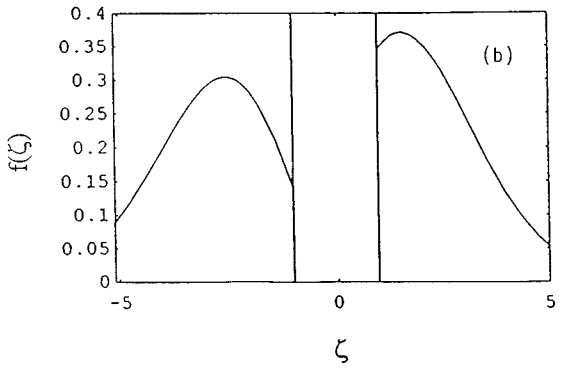

FIG. 7. (a) PDF for the $d=2$ problem with $\Gamma=0.1$ and $W=0.25$. (b) A cut of the PDF along the ζ axis.

We remark that the physical meaning of this PDF is slightly different from that found in Weiss, Kopelman, and Havlin [2] or in Taitelbaum [4]. Since in the absence of a field the distribution is angle independent, these authors define $f(L)$ as the PDF of the distance from the trap to the nearest mobile particle, regardless of the direction.

Using $f(L,\Omega)$, we could also evaluate the mean (dimensionless) distance from the center of the trap to the nearest neighbor in the direction Ω,

$$\langle L(\Omega)\rangle=\int_1^\infty Lf(L,\Omega)dL=\int_1^\infty\Phi(L,\Omega)dL. \tag{27}$$

For a perfect trap, the PDF vanishes at the trap boundary, but $f(1,\Omega)$ increases monotonically as Γ decreases. Cuts of $f(L,\Omega)$ along the field axis in the two-dimensional case are shown in Figs. 6, 7(b), and 8(b) for $\Gamma=0.1$, and the values of W indicated in the captions. Contour plots for the PDF are displayed in Figs. 7(a)–8(a).

Figure 6 corresponds to the almost complete absence of drift. The PDF has a minimum at the trap edge and, in the

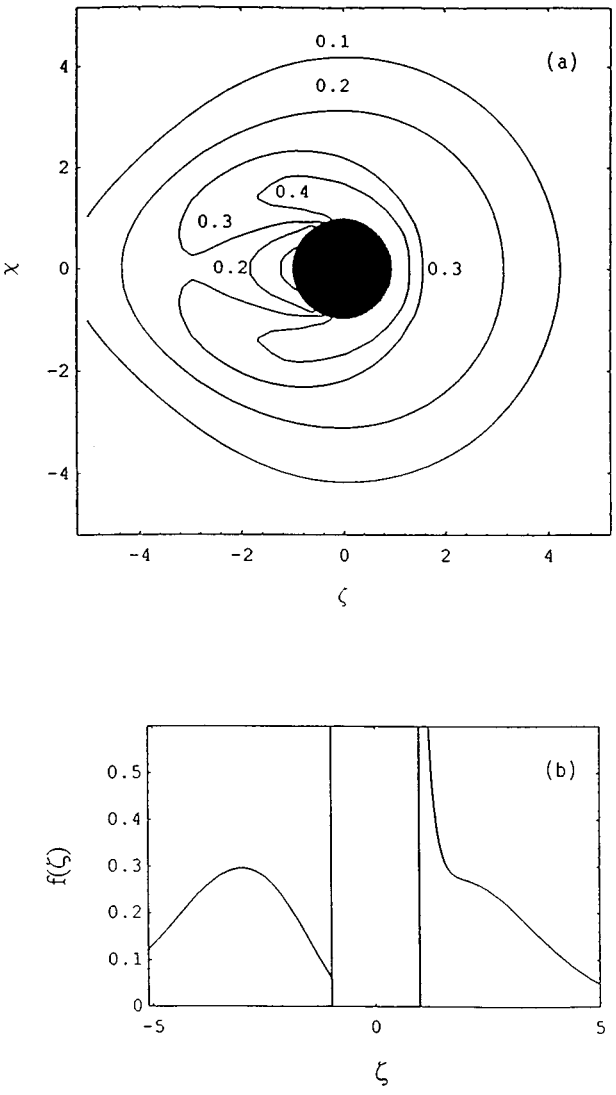

FIG. 8. (a) PDF for the $d=2$ problem with $\Gamma=0.1$ and $W=2.5$. (b) A cut of the PDF along the ζ axis.

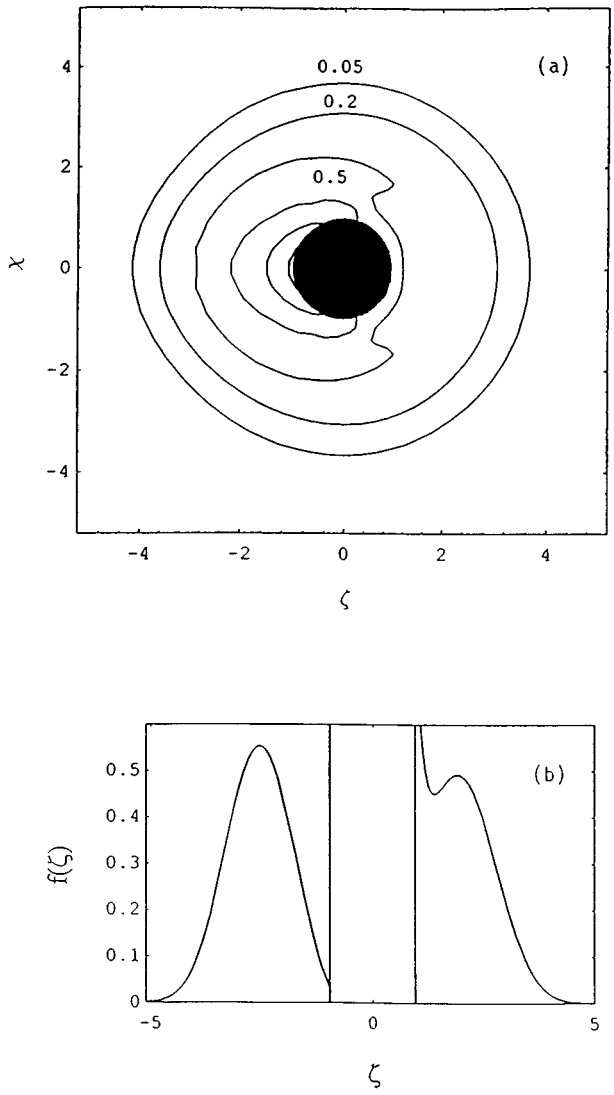

FIG. 9. (a) PDF for the $d=3$ problem with $\Gamma=0.1$ and $W=2.5$. (b) A cut of the PDF along the polar axis.

selected scale, looks completely symmetric. It agrees qualitatively with Taitelbaum's results for long (but finite) times [4]. However, if $W=0$ strictly, there is no field-induced replenishment of the depletion volume and the $f(L,t)$ maximum slowly moves to larger distances.

The effects of the field become evident in Figs. 7 and 8, where the asymmetry generated by the particle accumulation in front of the trap gives rise to a deformation of the high PDF annulus surrounding the trap. As the field is increased, the maximum that appears in front of the trap begins to strengthen and shift toward the trap. For intense fields the maximum is located at the trap edge, and a shoulder (Fig. 8) or a second maximum (if W is large enough) appears. This structure is due to the shape of $C_\infty(\xi,\theta)$ in front of the trap: From a maximum at $\xi=1$, it decays very fast with ξ, rapidly reaching a nonzero asymptotic value. As a consequence, the integral in Eq. (24) undergoes a rapid change as a function of L. The solid angle factor ξ^{d-1} contributes to the appearance of the shoulder (and, eventually, of a second maximum), its contribution being obviously stronger for higher dimensions. This can be appreciated in Fig. 9, which corresponds to a three-dimensional problem with a strong field, where we already observe a well-developed second maximum.

The field-induced modifications behind the trap are less striking. Since $C_\infty(\xi,\pi)$ increases monotonically with ξ, there is a minimum at $\xi=1$, and a rounded maximum at intermediate distances. For small W this maximum becomes stronger and moves toward the trap as we increase the field, but, for larger fields, this maximum eventually moves away from the trap and its height diminishes. We finish this section by remarking that, as was already noted, the perturbed volume becomes more compact for $d=3$, an important feature that is a direct result of the presence of more diffusion paths in higher dimensions.

VI. REACTION RATES

The steady-state particle flux into the trap contains both diffusive and convective contributions. It can be calculated as the radial component of the dimensionless current density at the trap surface,

$$J(\theta)=\frac{1}{C_0}[\vec{\nabla}C_\infty(\xi,\theta)+2\vec{W}C_\infty(\xi,\theta)]\cdot\vec{\eta}|_{\xi=1} \quad (28)$$

where $\hat{\eta}$ is a unit vector pointing radially inwards. For a perfect trap, $C_\infty(1,\theta)=0$ and $J(\theta)$ is computed directly as the radial derivative of the concentration evaluated at the trap boundary,

$$J(\theta)=\frac{1}{C_0}\frac{\partial}{\partial\xi}C_\infty(\xi,\theta)\bigg|_{\xi=1}. \quad (29)$$

Explicit results can be obtained for the two- and three-dimensional cases using Eqs. (13) and (23), respectively. For an imperfect trap, we can use Eq. (2) to obtain

$$J(\theta)=\frac{C_\infty(1,\theta)}{C_0}\Gamma. \quad (30)$$

The total trapping (or reaction) rate J can be found by integrating $J(\theta)$ over the whole trap surface. In the two-dimensional case, for a perfect trap, we obtain

$$J=\pi\sum_{j=0}^{\infty}(-1)^j\varepsilon_j^2I_j^2(W)\left[W\frac{K_{j+1}(W)}{K_j(W)}-j\right], \quad (31)$$

and, for an imperfect trap,

$$J=2\pi\Gamma\left[1+\sum_{j=0}^{\infty}(-1)^j\alpha_jI_j(W)K_j(W)\right]. \quad (32)$$

In the three-dimensional case, for a perfect trap, we obtain

$$J=1-\frac{\pi}{W}\sum_{j=0}^{\infty}(-1)^j(2j+1)I_{j+(1/2)}^2(W)\times\left[\frac{2j+1}{2}-W\frac{K_{j+(3/2)}(W)}{K_{j+(1/2)}(W)}\right], \quad (33)$$

and, for an imperfect trap,

$$J=4\pi\Gamma\left[1+\left(\frac{\pi}{2W}\right)^{1/2}\sum_{j=0}^{\infty}(-1)^j\alpha_jI_{j+1/2}(W)\times K_{j+(1/2)}(W)\right]. \quad (34)$$

The steady-state reaction rates are plotted as functions of the drift speed in Figs. 10 and 11 for the two- and three-dimensional cases, respectively. They increase monotonically with both Γ and W, as they should. In the $W\to0$ limit, $J\to0$ if $d=2$, but it goes to a nonzero limit if $d=3$, in agreement with Refs. [2] and [3]. For large fields, the problem becomes convection controlled, and the relative influence of diffusion weakens. Since the mobile particles can be absorbed only as fast as they reach the trap neighborhood, the high-field reaction rates have the form

$$J(W\to\infty)=G(\Gamma)\sigma W, \quad (35)$$

where σ is the trap cross section and G is an increasing function of Γ, which satisfies $G(0)=0$ (perfect reflector) and $G(\infty)=1$ (perfect trap). These results have been confirmed by numerical studies at speeds higher than those appearing in the graphs.

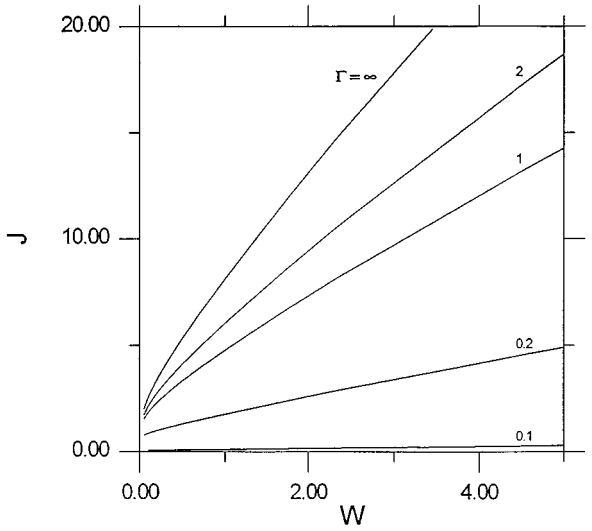

FIG. 10. Total reaction rate at the trap as a function of drift velocity for the $d=2$ problem. The values of Γ are indicated next to the corresponding curves.

VII. SMALL-FIELD LIMIT

As an application of the method introduced in Sec. IV, we next calculate the steady-state concentration for an imperfect trap in the small-field limit. We start with the two-dimensional case, which is specially interesting due to the absence of a steady state if $W=0$. Keeping only terms up to order W in Eqs. (11) and (17), we can solve Eq. (16) approximately to obtain the eigenfunction expansion coefficients α_j. The approximate values for B_i and M_{ij} are

$$B_0=\Gamma+O(W^2),$$
$$B_1=(\Gamma-2)W+O(W^3), \quad (36)$$
$$B_i\sim O(W^i)$$

and

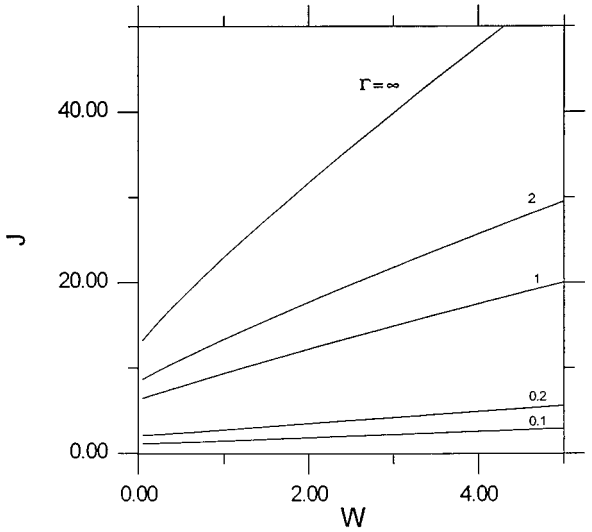

FIG. 11. Total reaction rate at the trap as a function of drift velocity for the $d=3$ problem. The values of Γ are indicated next to the corresponding curves.

$$M_{i,i}=-(i+\Gamma)\frac{(i-1)!}{2}\left(\frac{W}{2}\right)^{-i},$$
$$M_{i,i+1}=\frac{i!}{2}\left(\frac{W}{2}\right)^{-i}, \tag{37}$$
$$M_{i+1,i}=\frac{(i-1)!}{2}\left(\frac{W}{2}\right)^{-i+1},$$

with

$$M_{0,0}=-1+\Gamma[\ln(W/2)+\gamma],$$
$$M_{0,1}=\tfrac{1}{2}, \tag{38}$$
$$M_{1,0}=-W[\ln(W/2)+\gamma].$$

After substituting these expressions into Eq. (16), it is easy to see that the coefficients α_i must tend to zero at least as fast as W^{2i}. Therefore, by solving the reduced matrix equation, we find

$$\alpha_0=\frac{\Gamma}{\Gamma[\ln(W/2)+\gamma]-1},$$
$$\alpha_i\sim O(W^{2i}). \tag{39}$$

Finally, we obtain the steady-state concentration

$$C_\infty(\xi)=C_0\left(1-\frac{\gamma+\ln(W\xi/2)}{\gamma+\ln(W/2)-1/\Gamma}\right). \tag{40}$$

This equation is valid in the region $\xi\ll W^{-1}$, which becomes arbitrarily large as $W\to 0$. Note that, in this approximation, the problem is isotropic; the θ dependence is introduced in the next term of the expansion. Using Eq. (30) we can now obtain the total reaction rate

$$J=-\frac{2\pi}{\ln(W/2)+\gamma-1/\Gamma}. \tag{41}$$

For a given (small) value of W the reaction rate is an increasing function of Γ, as it should. Again the W dependence is logarithmic, again pointing to the marginality of the two-dimensional problem.

A similar calculation for the steady-state concentration in three dimensions yields

$$\alpha_0=-\frac{2\Gamma}{\Gamma+1}\left(\frac{W}{2\pi}\right)^{1/2}+O(W^{7/2}),$$
$$\alpha_i\sim O(W^{2i+1/2}). \tag{42}$$

We then obtain the weak-field form of the concentration,

$$C_\infty(\xi,\theta)\sim C_0\left[1-\frac{\Gamma}{(\Gamma+1)\xi}\left(1+\frac{W\cos\theta}{\Gamma(\Gamma+2)\xi}\times(2\Gamma^2-4+\Gamma(\Gamma+2)\xi^2)\right)\right] \tag{43}$$

($\xi\ll W^{-1}$), and of the total reaction rate,

$$J=\frac{4\pi\Gamma}{\Gamma+1}\left[1-W^2\frac{2}{3}\frac{\Gamma^2-2}{\Gamma+2}\right]. \tag{44}$$

It is evident that these asymptotic results agree with those of Taitelbaum and co-workers [3,4]. Of course, the reaction rate is a monotonically increasing function of Γ. It goes to a finite nonzero value in the absence of drift.

VIII. CONCLUSIONS

We have performed a detailed study of the steady state of a diffusion-controlled reaction occurring in a two- or three-dimensional space, where one species consists of mobile reactants diffusing under the influence of a uniform field, while the other species behaves as a set of fixed (perfect or imperfect) traps. Although in the absence of a field there is no steady state in two dimensions, the addition of the weakest field will eventually drive the system to a steady state. We have described the steady-state distribution of particles in the trap neighborhood, showing that an enhanced concentration (depletion) region usually arises upstream (downstream) an imperfect trap. We have also analyzed the dependence of the reaction rates and of the probability distribution function for the first neighbor with field and trap strength. Our results show that the volume of the perturbed region decreases when the problem dimensionality is increased.

Since no completely analytic treatment is possible for imperfect traps, we introduced a simple matrix method that led to (a) approximate expressions in the small-field limit, and (b) reliable numerical results for arbitrary values of the parameters. We stress that anybody interested can follow this method to obtain results for any desired set of parameters with a minimum of numerical work (the required matrix inversion can be performed by any mathematics software on a personal computer in a matter of seconds).

ACKNOWLEDGMENTS

This research was supported by PID/CONICOR Grant No. 3232/94, and by the National Science Foundation through Grant No. HRD-9450342. C.A.C. wishes to thank the Facultad de Matemática, Astronomía y Física at Universidad Nacional de Córdoba for its hospitality.

[1] D. Ben-Avraham and G. H. Weiss, Phys. Rev. A **39**, 6436 (1989).
[2] G. H. Weiss, R. Kopelman, and S. Havlin, Phys. Rev. A **39**, 466 (1989).
[3] H. Taitelbaum. R. Kopelman, G. H. Weiss, and S. Havlin, Phys. Rev. A **41**, 3116 (1990).
[4] H. Taitelbaum, Phys. Rev. A **43**, 6592 (1991).
[5] M. von Smoluchowski, Ann. Phys. (Leipzig) **48**, 1103 (1915).

[6] F. C. Collins and G. E. Kimball, J. Colloid Sci. **4**, 425 (1949).
[7] P. J. Schultz and K. G. Lynn, Rev. Mod. Phys. **60**, 701 (1988).
[8] H. Nakajima and H. B. Huntington, J. Phys. Chem. Solids **42**, 171 (1981).
[9] H. K. Pak and B. M. Law, Europhys. Lett. **31**, 19 (1995).
[10] J. R. Philip, J. H. Knight, and R. T. Waechter, Water Resour. Res. **25**, 16 (1989).
[11] J. H. Knight, J. R. Philip, and R. T. Waechter, Water Resour. Res. **25**, 29 (1989).
[12] F. J. Alexander and J. L. Lebowitz, J. Phys. A **27**, 683 (1994).
[13] C. A. Condat, G. Sibona, and C. E. Budde, Phys. Rev. E **51**, 2839 (1995).
[14] B. Y. Balagurov and V. G. Vaks, Zh. Éksp. Teor. Fiz. **65**, 1939 (1973) [Sov. Phys. JETP **38**, 968 (1974)].
[15] P. Grassberger and I. D. Procaccia, Phys. Rev. A **26**, 3686 (1982).
[16] C. A. Condat and D. P. Prato, Phys. Lett. A **180**, 388 (1993).
[17] H. S. Carslaw and J. C. Jaeger, *Conduction of Heat in Solids*, 2nd ed. (Oxford University Press, Oxford, 1986).
[18] *Handbook of Mathematical Functions*, edited by M. Abramowitz and I. Stegun (Dover, New York, 1965).
[19] Ch. R. Doering and D. Ben-Avraham, Phys. Rev. A **38**, 3035 (1988).
[20] S. Redner and D. Ben-Avraham, J. Phys. A **23**, L1169 (1990).